

Quintessence and Thermal Matter

S. Hsu^{*}, B. Murray[†]

Department of Physics

University of Oregon, Eugene OR 97403-5203

November 4, 2018

Abstract

We investigate the effects of thermal interactions on tracking models of quintessence. We show that even Planck-suppressed interactions between matter and the quintessence field can alter its evolution qualitatively. The dark energy equation of state is in many cases strongly affected by matter couplings. We obtain a bound on the coupling between quintessence and relativistic relic particles such as the photon or neutrino.

^{*}hsu@duende.uoregon.edu

[†]bmurray1@darkwing.uoregon.edu

1 Introduction

Recent evidence [1] suggests that a large fraction of the energy density of the universe has negative pressure, or equation of state with $w \equiv p/\rho < 0$. One candidate source of this dark energy is a slowly varying and spatially homogeneous scalar field called quintessence [2]. Because the dark energy redshifts more slowly than ordinary matter or radiation, it appears that the ratio of energy density of quintessence to that in ordinary particles must be fine tuned to a specific infinitesimal value in the early universe in order to explain its current observed value. One class of models that ameliorate this problem describe *tracker fields* [3] whose evolution is largely insensitive to initial conditions and at late times begin to dominate the energy density of the universe with a negative equation of state. Tracker models have difficulty producing w_ϕ consistent with observational data: they generally imply $w_\phi^{\text{eff}} \gtrsim -0.7$, whereas WMAP implies $w_\phi^{\text{eff}} < -0.78$ (95% CL) [1]. (Here, effective means as measured observationally, so integrating over redshifts less than of order 10^3 .) Nevertheless, they provide an interesting class of models describing dark energy as a slowly evolving scalar field. An alternative class of models, which avoids the extremely flat potentials required at late times of tracker models, utilizes nonlinear field oscillations that exhibit $w < 0$ [4].

Tracker models generally require only a single adjustable parameter. Once this parameter is appropriately chosen, a wide range of initial values of the tracker field, ϕ , and its derivative, $\dot{\phi}$, result in similar values of its energy density today. This is due to an attractor-like property of the tracker equations of motion.

In this paper we investigate the effects of interactions between the quintessence field, ϕ , and ordinary matter particles in the early universe. It is important to note that while the zero temperature potential may be fine tuned in order for the evolution of ϕ to have the attractive properties mentioned above, the same may not be done with the finite temperature effective potential. That is to say, once the form of the renormalized zero temperature potential is determined, no additional freedom remains to fine-tune away unwanted thermal effects. Therefore, such effects must be considered. We expect thermal interactions to be at least of gravitational strength (even in the case where ϕ is a “hidden sector” field). At minimum, quantum gravity is likely to produce interactions of the type [5]

$$\frac{\beta_i}{M_P} \phi \mathcal{L}_i \quad , \quad (1)$$

where M_P is the Planck scale, and \mathcal{L}_i are terms in the standard model lagrangian, including for example

$$F_{\mu\nu}^2 \quad , \quad F_{\mu\nu} \tilde{F}^{\mu\nu} \quad , \quad \bar{\psi} \not{D} \psi \quad , \quad \dots$$

where F is the field strength of any gauge field (including the photon, but not excluding

gluons or the W or Z) and ψ is any fermion field from neutrinos to the top quark. Even if ϕ were a pseudo-Goldstone boson [6], it would be surprising not to find at least Planck-suppressed violations of the resulting $\phi \rightarrow \phi + \text{constant}$ symmetry. String theory, for example, is believed to not exhibit any exact global symmetries [7]. Previous constraints on certain β_i are quite strong, where the coupling is to the photon or gluon [6]. However, some β_i could be much larger, such as when the interaction is with the W, Z or even a neutrino¹.

In the early universe matter particles are in thermal equilibrium, and the interactions in (1) produce a thermal mass for ϕ of the form

$$\left(\frac{\beta_i}{M_P}\right)^2 \phi^2 T^4, \quad (2)$$

where T is the temperature. If the thermal degree of freedom is massive, the thermal effect goes to zero exponentially as $e^{-m/T}$ when the temperature drops below the mass m . We note that the thermal effects of interest here are *in addition* to any quantum corrections to the effective potential resulting from the interactions between matter and quintessence (see, for example, [9]). In general, the bare parameters of quintessence models must be fine-tuned in order to obtain potentials of the necessary type. We assume here that this fine-tuning is achieved (whatever its consequences for the plausibility of the model) and focus on thermal effects which must also arise.

Although ϕ may not itself be in equilibrium, nevertheless its dynamical evolution will be affected by these thermal interactions, just as for the axion field near the QCD phase transition [10]. We can derive the correction (2) to the effective potential for ϕ as follows. Let the cold ϕ field be a static, external source for a Euclidean path integral describing the thermal degrees of freedom. The timelike boundary conditions for the path integral have period given by the inverse temperature. Performing the integration over the thermal fields yields a contribution to the effective potential for ϕ , and the usual perturbative analysis identifies the leading effect to be the thermal mass term in (2). In this calculation, we need never assume that ϕ itself is in thermal equilibrium, yet its effective potential receives temperature-dependent contributions.

In what follows we will examine how the contribution of (2) to the tracker potential modifies its evolution. We can make a simple argument for why (2) is non-negligible at late times. At late times, the quintessence field must have a very small mass: $V''(\phi)^{1/2} \lesssim H_0 \sim 10^{-33}$ eV, and contribute of order closure density to Ω : $V(\phi) \sim (10^{-33}\text{eV})^4$, which implies that $\phi \sim M_P$. This means that the mass term in (2) can be roughly the same size as $V(\phi)$, up to powers of β_i .

¹Direct coupling to relic neutrinos has been considered previously [8].

At early times, (2) also affects the evolution in many cases. Suppose the tracker potential is given by $V(\phi) = M^{l+4}\phi^{-l}$, where $l > 4$. Then $V(\phi_*)$ and (2) are comparable at the minimum of the combined potential:

$$\phi_* \sim M \left(\frac{M^2 M_P^2}{\beta^2 T^4} \right)^{\frac{1}{l+2}}, \quad (3)$$

where the potential energy density is roughly

$$V(\phi_*) \equiv V_* \sim M^4 \left(\frac{\beta^2 T^4}{M^2 M_P^2} \right)^{\frac{l}{l+2}}. \quad (4)$$

In many cases, ϕ oscillates about the temperature-dependent minimum ϕ_* . The oscillation energy redshifts faster than the potential energy at the minimum, $V_* \sim T^{4l/(l+2)}$, so ϕ simply tracks ϕ_* with oscillations that decrease in amplitude over time. Interestingly, V_* redshifts exactly as the energy density of the tracker solution [11] (assuming radiation domination; during a matter dominated epoch V_* redshifts somewhat faster than the usual tracker energy density). This means that thermal effects will keep ϕ and its energy density near their desired values, even though the physics responsible is very different. When the thermal term eventually either disappears due to the crossing of a particle mass threshold, or becomes negligible due to redshift, ϕ will merge back to a tracker solution.

2 Evolution results

We assume a spatially flat Robertson-Walker universe, with metric $ds^2 = dt^2 - a^2(t)d\mathbf{x}^2$. The evolution of a scalar field minimally coupled to gravity in this spacetime is given by the Klein-Gordon equation:

$$\ddot{\phi} + 3H\dot{\phi} + V'(\phi) = 0, \quad (5)$$

where a dot denotes the derivative with respect to cosmic time, and a prime denotes the derivative with respect to ϕ . The evolution of the scale factor is governed by the Friedmann equation:

$$H^2 = \left(\frac{\dot{a}}{a} \right)^2 = \frac{8\pi}{3M_P^2} (\rho_m + \rho_r + \rho_\phi), \quad (6)$$

where if z denotes the redshift, then $\rho_m = \rho_c \Omega_m (1+z)^3$, $\rho_r = \rho_c \Omega_r (1+z)^4$, and $\rho_\phi = \frac{1}{2}\dot{\phi}^2 + V(\phi)$. Here the subscript m refers to both baryons and cold dark matter, and the subscript r refers to both photons and neutrinos. If the universe is spatially flat, then it will always be the case that $\Omega_m + \Omega_r + \Omega_\phi = 1$. Observational data [1] currently favor $\Omega_m \sim 0.3$, $\Omega_r \sim 10^{-4}$ and $\Omega_\phi \sim 0.7$.

Equations (5) and (6) were integrated numerically for a wide range of ϕ_i and $\dot{\phi}_i$ from an initial redshift of $z_i = 10^{28}$ (temperature $\sim 10^{16}$ GeV), which might plausibly correspond to the end of inflation. Motivated by the arguments of the previous section, we took $V(\phi)$ to be

$$V(\phi) = M^{4+l}\phi^{-l} + \left(\frac{\beta}{M_P}\right)^2 \phi^2 T^4, \quad (7)$$

where $l > 4$, β is a free parameter, and M is constrained such that $\Omega_\phi \sim 0.7$. For example, for $l = 6$ and $\beta = 0$, $M \sim 4.7 \times 10^6$ GeV. In this simulation, $T(z) \equiv \sqrt[4]{\rho_r} = \sqrt[4]{\rho_c \Omega_r}(1+z)$ (we are not precise about the number of relativistic degrees of freedom). It is worth noting that, since the second term in (7) arises due to a loop effect, it should actually appear in (7) multiplied by a constant of order 10^{-1} . In the absence of this factor, the quantity β in (7) differs somewhat from the β_i in (1). This consideration, however, has no effect on the qualitative picture described below.

Based on our simulations, we make the following observations.

For $\beta = 0$, tracking occurs for a large range of initial conditions in ϕ and $\dot{\phi}$, as described in [3]. In particular, for $l = 6$, if ϕ starts from rest, any ϕ_i in the range $10^{-18}M_P \lesssim \phi_i \lesssim 10^{-2}M_P$ will be on track by today. In general, the limits for ϕ_i that will be on track by today, assuming $\dot{\phi}_i = 0$, are found by solving $\rho_{\phi i} = M^{l+4}\phi_i^{-l}$ for ϕ_i , where $\rho_{\phi i}$ is the initial energy density in ϕ . By noting that $M \sim (\rho_{\phi o}M_P^l)^{1/(4+l)}$, where $\rho_{\phi o}$ is the present energy density in ϕ , it is straightforward to see that these limits on ϕ_i depend on l :

$$\phi_i \sim M_P \left(\frac{\rho_{\phi o}}{\rho_{\phi i}}\right)^{\frac{1}{l}}. \quad (8)$$

The minimum value of ϕ_i that will be on track by today, $\phi_{i,min}$, is then simply found by setting $\rho_{\phi i}$ equal to its maximum value. For an initial redshift of 10^{28} , this corresponds roughly to $\rho_{\phi i} \sim 10^{-4}\rho_{Bi}$, where ρ_{Bi} is the energy density of dominant background component, radiation at this redshift ($\rho_r(z = 10^{28}) \sim 10^{61}$ GeV⁴). Similarly, the maximum value of ϕ_i that will be on track by today, $\phi_{i,max}$, is found by setting $\rho_{\phi i}$ equal to its minimum value, which is roughly the background energy density at equality, $\rho_{eq} \sim 10^{-37}$ GeV⁴.

For $\beta \neq 0$, $\phi_{i,min}$ is essentially unchanged because the first term in (7) is dominant for $\rho_{\phi i} \sim 10^{-4}\rho_{Bi}$, unless β is made very large ($\beta \sim 10^{20}$). β this large will not be discussed further in this paper. For sufficiently small β , $\phi_{i,max}$ is also left unchanged. Let $\beta_c \equiv (10^{-4})^{1/2}(\rho_{eq}/\rho_{\phi o})^{1/l} \sim 10^{(11-2l)/l}$. Then for $\beta = \beta_c$ and $\phi_i = \phi_{i,max}$, $\rho_{\phi i} = 10^{-4}\rho_{Bi}$. But $\rho_{\phi i} \leq 10^{-4}\rho_{Bi}$, and $\rho_\phi \propto \beta^2\phi^2$ for $\phi \gg \phi_*$. Therefore, for $\beta \gtrsim \beta_c$, $\phi_{i,max} \propto 1/\beta$. The net result is that the range of ϕ_i that will be on track by today (with $\dot{\phi}_i = 0$) is independent of β for $\beta \lesssim \beta_c$ and goes like $1/\beta$ for $\beta \gtrsim \beta_c$.

In addition to affecting the range of ϕ_i that track, the choice of β qualitatively affects

the dynamics of ϕ . Note that $10^{-2} \lesssim \beta_c \lesssim 1$. In examining the dynamics of ϕ there again seems to be a critical value of β . Although this critical value seems to be $\sim 10^{-1}$, it is not clear whether it is equal to β_c . As mentioned above, a factor of order 10^{-1} was not included in (7). Therefore, in what follows reference will be made to β_c , which is meant to indicate a β in the range $10^{-2} \lesssim \beta \lesssim 1$.

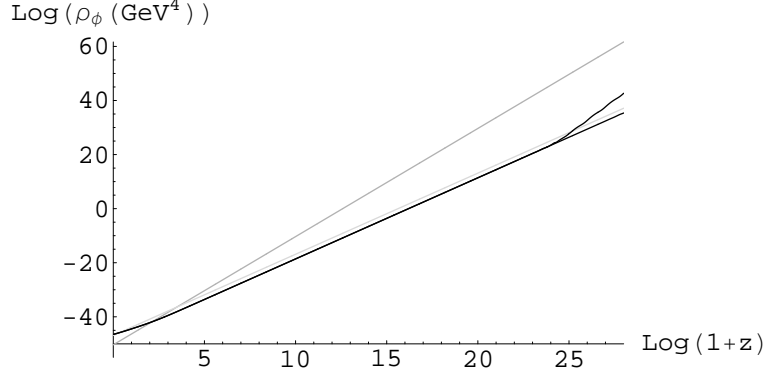


FIG. 1. The evolution of ρ_ϕ is shown for $\beta = 3$, $l = 6$ and an intermediate $\rho_{\phi i}$ ($\phi_i \ll \phi_{*i}$). ρ_ϕ for $\phi_i = \phi_{*i}$ (corresponding to the tracker solution for $\beta = 3$) is also plotted for reference, as are ρ_r (medium gray) and ρ_m (light gray). Note that ρ_ϕ cannot decrease below the energy density of the tracker solution (it is always larger than V_*) and subsequently freeze as it does for $\beta = 0$. Also, note that, at high redshift, small oscillations can be seen in ρ_ϕ corresponding to oscillations of ϕ about ϕ_* (as in Figure 2).

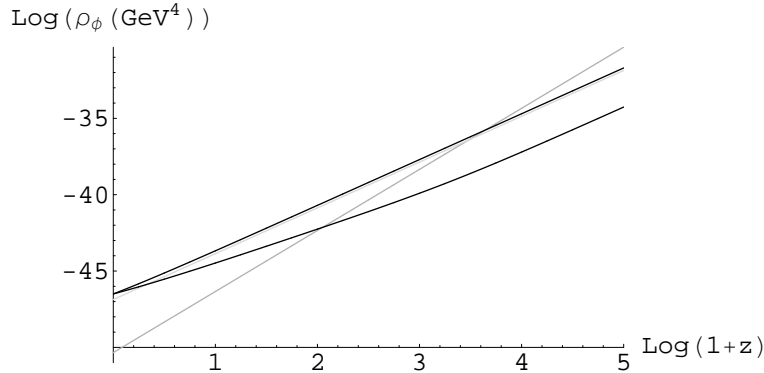


FIG. 2. The late time behavior of the tracker solution is shown for $\beta = 0$ (lower curve) and $\beta = 10^2$ (upper curve) with $l = 6$. Again ρ_r (medium gray) and ρ_m (light gray) are plotted for reference. Note that while $\rho_\phi(\beta = 0)$ has a rather shallow slope today, $\rho_\phi(\beta = 10^2)$ cannot because $\rho_\phi > V_*$, and $V_*(\beta = 10^2) > \rho_m$. Also, note that the redshift at which ρ_ϕ begins to dominate depends on β .

For $\beta \lesssim \beta_c$, the behavior of $\phi(z)$ is essentially just that described in [3], with the one additional constraint that $\rho_\phi(z) > V_*(z)$, at all times (see Figures 1 and 2). For $\beta \gtrsim \beta_c$,

$\phi(z)$ oscillates about $\phi_*(z)$ (see Figure 3). The period of these oscillations in $\phi(z)$ decreases exponentially with the scale factor, while the amplitude decreases monotonically, but not exponentially, per se. As either side of the potential (7) are made steeper; i.e., either l or β are increased, the period of oscillation decreases, as does the amplitude. The fact that these oscillations have been damped out by today and that V_* redshifts at the same rate (for RD) or faster (for MD) than the tracker solution is what allows for tracking to occur, even with $\beta \gtrsim \beta_c$. Adding extra terms to (7), which cause V_* to redshift slower than the tracker solution during RD will be discussed below in Section 3.

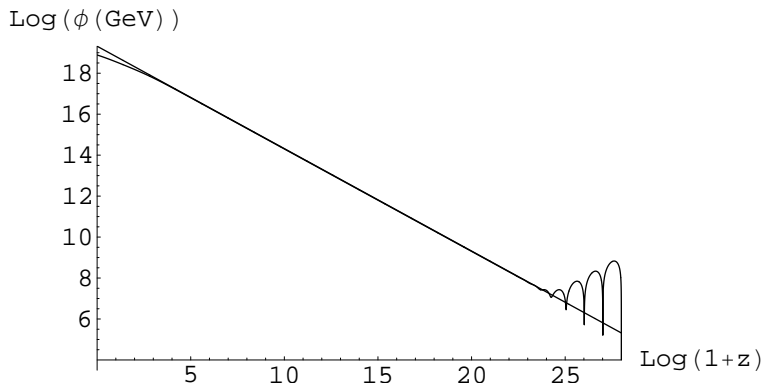


FIG. 3. The evolution of ϕ is shown for $\beta = 3$, $l = 6$ and an intermediate $\rho_{\phi i}$ ($\phi_i \ll \phi_{*i}$). ϕ_* is also plotted for reference. Note that ϕ oscillates about ϕ_* at large redshift; ϕ follows ϕ_* closely for most of its evolution, but for small redshift it begins to fall behind.

For $\beta \lesssim \beta_c$, the scale M in (7) is simply equal to its value for $\beta = 0$; i.e., $M \sim (\rho_{\phi o} M_P^l)^{1/(4+l)}$. For $\beta \gtrsim \beta_c$, M slowly decreases as β is increased, e.g. for $l = 6$ and $\beta = 0$, $M \sim 4.7 \times 10^6$ GeV, whereas for $l = 6$ and $\beta = 10^3$, $M \sim 1.0 \times 10^6$ GeV.

We define the scalar field equation of state:

$$w_\phi \equiv \frac{1+z}{3\rho_\phi} \frac{d\rho_\phi}{dz} - 1 \quad . \quad (9)$$

The definition (9) coincides with the usual definition of the scalar field equation of state:

$$w_\phi^{\text{usual}} \equiv \frac{p_\phi}{\rho_\phi} = \frac{\frac{1}{2}\dot{\phi}^2 - V(\phi)}{\frac{1}{2}\dot{\phi}^2 + V(\phi)} \quad (10)$$

as a consequence of energy conservation. However, because we did not take into account the back reaction on matter and radiation of the ϕ interaction, there are regimes in our simulation where (9) differs from (10). To be precise, we have treated ordinary matter as a thermal background, and have not accounted for energy flowing from ϕ into the heat bath. This is generally a negligible effect, except when the dark energy density is large and ϕ

is of order M_P , which can occur at late times. The evolution of ϕ can strongly influence the thermal matter (for example, changing the coefficient of its kinetic term), which we have not accounted for. The late time behavior of our simulations at large β is therefore only qualitatively and not quantitatively correct. Observational probes such as WMAP are sensitive to the way the dark energy density redshifts, and hence constrain (9).

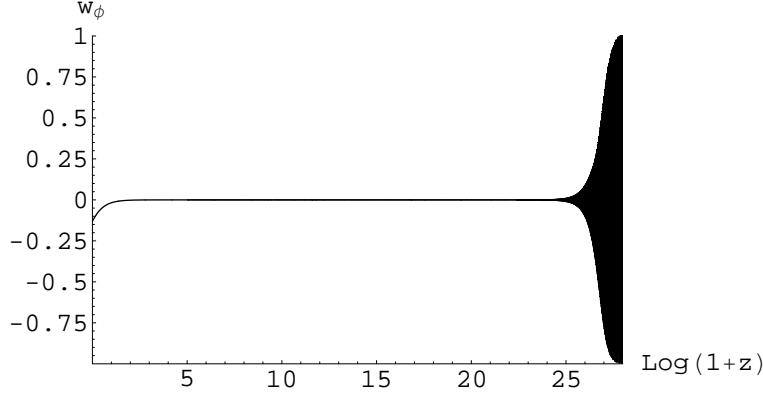


FIG. 4. The evolution of w_ϕ is shown for $\beta = 10^2$, $l = 6$ and an intermediate $\rho_{\phi i}$ ($\phi_i \ll \phi_{*i}$). Note that the (very rapid) oscillations in w_ϕ (corresponding to oscillations of ϕ about ϕ_*) are completely damped out very early in the evolution of ϕ , and that $w_\phi \sim 0$ for most of the evolution of ϕ . Also, note that today $w_\phi \sim -0.13$, compared to the $\beta = 0$ value of $w_\phi \sim -0.4$.

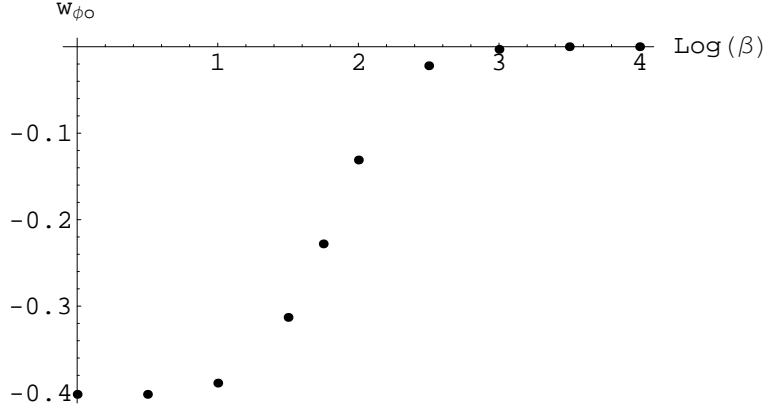


FIG. 5. The present value of w_{ϕ_0} is plotted versus $\log(\beta)$ for $l = 6$. Note that for $\beta \gtrsim 10$, w_{ϕ_0} begins to deviate from its $\beta = 0$ value. For $\beta \gtrsim 10^3$, $w_{\phi_0} \sim 0$.

For $\beta \gtrsim \beta_c$, there are oscillations in w_ϕ , corresponding to the oscillations seen in ϕ (see Figure 4). Again, the period of these oscillations decreases as β is increased, and the period decreases exponentially with the scale factor. By increasing l , the present value of w_ϕ is driven toward zero (from below). By increasing β (beyond $\sim \beta_c$), w_{ϕ_0} is also driven towards zero (see Figure 5), as the evolution of ϕ becomes controlled by ϕ_* , and the energy density

by V_* . In the extreme limit ϕ tracks ϕ_* closely and its energy is almost entirely potential, rather than kinetic. Note that $-1 < w_\phi < 0$ at late times for all l and β .

For $\beta = 0$ and $l = 6$, $w_{\phi o} \sim -0.4$. In general, if a sum of inverse powers of ϕ are allowed, then $w_\phi^{\text{eff}} > -0.7$ [3]. This is the effective equation of state measured by supernovae and microwave background experiments, which integrate over a (potentially) varying w_ϕ . This bound represents the best case scenario for $\beta = 0$ tracker models, in that it is most consistent with observational data for w_ϕ^{eff} , which put $w_\phi^{\text{eff}} < -0.78$ (95% CL) [1]. The inclusion of the second term in (7) with sufficiently large β ($\beta \gtrsim \beta_c$) results in $\phi \simeq \phi_*$ throughout most of its evolution. For $l = 6$, this yields an equation of state, $w \sim 0$ (since $V_* \sim T^3$), that is even further from the observational bound (see Figure 5). At very late times, ϕ does not increase sufficiently rapidly to stay near ϕ_* (see Figure 3). Instead, it rejoins a tracker solution and its equation of state reverts to one in which the energy density redshifts more slowly than V_* (see Figure 2).

3 Discussion

Our analysis shows that the evolution of the tracker field depends quite sensitively on its interaction with thermal matter, even when the strength of the couplings is as small as one would imagine they may possibly be; i.e., Planck-suppressed. When β is larger than of order unity, there is a tendency for the evolution to be controlled by that of ϕ_* , once initial oscillations have damped away. By a lucky coincidence, the redshift of $V_* \sim T^{4l/(l+2)}$ is the same as that of the tracker solution (during radiation domination), so that ϕ can rejoin a tracker solution at late times. The most dangerous possibility (which is realized when $\beta \gtrsim \beta_c$) is that ϕ is still following ϕ_* at late times, in which case its equation of state will be far from the observationally favored $w_\phi = -1$. For general l , the equation of state obeyed by V_* is $w_{\phi*} = (l - 6)/3(l + 2)$, which is never consistent with observational bounds for $l > 4$. We have checked that the behavior described above is qualitatively similar when higher order terms such as

$$\left(\frac{\beta}{M_P}\right)^3 \phi^3 T^4 \quad (11)$$

are included in the potential.

Hence, we conclude that there are stringent limits on the coupling between the tracker field and any particles which are still relativistic today, such as the photon or neutrinos. Such limits cannot be avoided through fine tuning of the finite temperature effective potential; once the zero temperature potential has been computed the finite temperature effects are determined. Interactions which are more than roughly two orders of magnitude stronger

than Planck-suppressed lead to a problematic equation of state. Couplings of the tracker to heavy particles, which freeze out at $T \sim m$, may alter the tracker evolution at early times, but do not affect the observed dark energy equation of state and are hence poorly constrained. The best hope of directly detecting the quintessence field may be through its interaction with massive particles.

Finally, although our analysis has focused on tracker models, similar results apply for any quintessence model in which the field is today slowly evolving in a very flat potential. As we argued in the introduction, in *any* such model the value of ϕ must be of order M_P today, which means that thermal terms such as (2) or (11) will be important for sufficiently large β . Large couplings to relic particles such as neutrinos can be ruled out as they lead to a problematic equation of state.

Acknowledgements

The work of S.H. and B.M. was supported in part under DOE contract DE-FG06-85ER40224.

References

- [1] For a determination of cosmological parameters from WMAP data, see D.N. Spergel, et al., *Astrophys. J. Suppl.* **148**, 175 (2003), astro-ph/0302209.
- [2] For a review of dark energy and quintessence, see, e.g., P.J. Peebles and B. Ratra, *Rev. Mod. Phys.* **75**, 559 (2003), astro-ph/0207347; T. Padmanabhan, *Phys. Rept.* **380**, 235 (2003), hep-th/0212290.
- [3] I. Zlatev, L.M. Wang and P.J. Steinhardt, *Phys. Rev. Lett.* **82**, 896 (1999), astro-ph/9807002; P.J. Steinhardt, L.M. Wang and I. Zlatev, *Phys. Rev. D* **59**, 123504 (1999), astro-ph/9812313; P. Brax and J. Martin, *Phys. Rev. D* **61**, 103502 (2000), astro-ph/9912046.
- [4] V. Sahni and L.M. Wang, *Phys. Rev. D* **62**, 103517 (2000), astro-ph/9910097; S.D.H. Hsu, *Phys. Lett. B* **567**, 9 (2003), astro-ph/0305096.
- [5] M. Kamionkowski and J. March-Russell, *Phys. Rev. Lett.* **69**, 1485 (1992), hep-th/9201063; R. Holman, S.D.H. Hsu, E.W. Kolb, R. Watkins and L.M. Widrow, *Phys.*

- Rev. Lett. **69**, 1489 (1992); R. Holman, S.D.H. Hsu, T.W. Kephart, E.W. Kolb, R. Watkins and L.M. Widrow, Phys. Lett. B **282**, 132 (1992), hep-ph/9203206; M. Kamionkowski and J. March-Russell, Phys. Lett. B **282**, 137 (1992), hep-th/9202003; S.M. Barr and D. Seckel, Phys. Rev. D **46**, 539 (1992); S. Ghigna, M. Lusignoli and M. Roncadelli, Phys. Lett. B **283**, 278 (1992).
- [6] S.M. Carroll, Phys. Rev. Lett. **81**, 3067 (1998), astro-ph/9806099.
- [7] J. Polchinski, *String Theory, Vol. 2: Superstring Theory And Beyond*, Cambridge Univ. Press, Cambridge, 1998.
- [8] R. Horvat, Mod. Phys. Lett. A **14**, 2245 (1999), hep-ph/9904451.
- [9] M. Doran and J. Jaeckel, Phys. Rev. D **66**, 043519 (2002), astro-ph/0203018.
- [10] For a explanation of axion dynamics, see, e.g., E.W. Kolb and M.S. Turner, *The Early Universe*, Westview Press (1994).
- [11] B. Ratra and P.J. Peebles, Phys. Rev. D **37**, 3406 (1988).